RSC Advances

ROYAL SOCIETY OF CHEMISTRY

www.rsc.org/advances

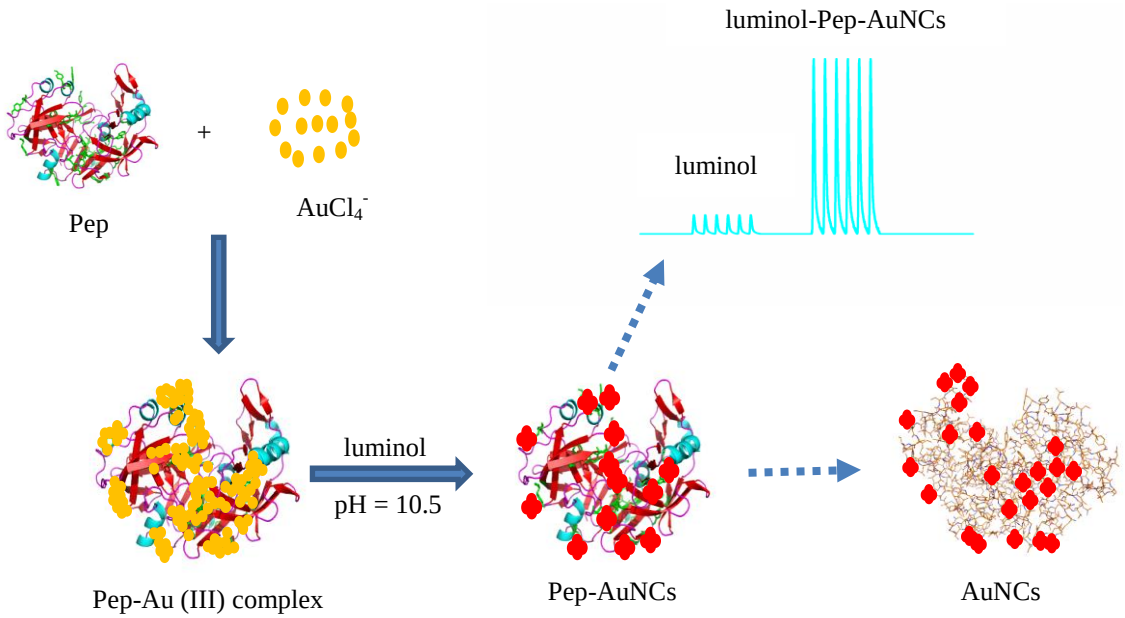

Study captopril pharmacokinetics in rabbit blood with microdialysis based on online generated Au nanoclusters and pepsin-captopril interaction in luminol chemiluminescence

Kai Luo[1], Fei Nie[1], Yumei Yan[2], Shixiang Wang[2], Xiaohui Zheng[2], Zhenghua Song[1]*

1. Key Laboratory of Synthetic and Natural Functional Molecule Chemistry of Ministry of Education, College of Chemistry & Material Science, Northwest University, Xi'an, 710069, China

2. Key Laboratory of Resource Biology and Biotechnology in Western China, College of Life Sciences, Northwest University, Xi'an 710069, China

*Corresponding author: Tel: (+86)029−88303798; Fax: (+86)029−88302604;

Email: songzhenghua@hotmail.com; zhsong123@nwu.edu.cn

Abstract

An ingenious luminol-$HAuCl_4$-pepsin (Pep) flow injection-chemiluminescence (FI-CL) system was explored to determine captopril (CAP) based on the CL intensity inhibited effect and applied to study CAP pharmacokinetic in rabbits with micro-dialysis. Interesting, $HAuCl_4$ and Pepsin (Pep) could significantly enhance the luminol chemiluminescence (CL) intensity. It was founded that sub-nanometer Au nanoclusters (AuNCs) were generated in the luminol-$HAuCl_4$-Pep reaction solution. The possible mechanism for AuNCs generated was given. By means of the FI-CL and molecular docking (MD) methods, the Pep-CAP interaction was systematically studied. The results showed that CAP might enter into Pep active site Asp32 with the binding constant (K) 1.7×10^6 $L \cdot mol^{-1}$, which could effectively inhibit the CL intensity. The CL intensity could be remarkably inhibited by CAP and the decrement of CL intensity was linear correlated to the logarithm of CAP concentrations in the range of 3.0 $pmol \cdot L^{-1}$ ~ 0.1 $\mu mol \cdot L^{-1}$ with a detection limit of 1.0 $pmol \cdot L^{-1}$ (3σ). This proposed approach was successfully applied to determine CAP in rabbit's blood during 16 h after intragastric administration with elimination ratio of 45.9% and recoveries ratio from 89.0% to 112.0%. The pharmacokinetic results showed that the CAP could be rapidly absorbed into blood with peak concentration (C_{max}) of 9.63 ± 1.45 $\mu g \cdot mL^{-1}$ at maximum peak time (T_{max}) of 0.75 ± 0.08 h; the elimination half-life of 3.19 ± 0.13 h and the elimination rate constant of 7.27 ± 0.41 $L \cdot g^{-1} \cdot h^{-1}$ in rabbits were derived, respectively.

Keywords: Chemiluminescence, Pepsin, $HAuCl_4$, Captopril, Micro-dialysis, Pharmacokinetics

Introduction

Protein-drug interaction has become a hot spot in the fields of medicine, chemistry and biology for drug discovering, screening, designing and developing [1-3]. Recently, numerous works have been performed on predicting the binding sites of drug to proteins and analyzing the interaction patterns between them [4, 5]. The Pepsin (Pep) (MW: 34.5 kD) is a monomeric, two domain, mainly *L*-protein, with a high percentage of acidic residues (43 out of 327) [6]. The catalytic sites are Asp32 and Asp215 for the Pep to be active [7]. The Pep, as a digestive protease, has the most efficiency for cleaving peptide bonds between hydrophobic and aromatic amino acids such as phenylalanine (Phe), tryptophan (Trp) and tyrosine (Tyr). The interaction behavior of Pep with bisphenol A [8], nobiletin [9] and fleroxacin [10] were systemically investigated by fluorescence spectroscopy, UV-visible absorption, resonance light scattering, synchronous fluorescence spectroscopy, 3D spectroscopy and molecule docking (MD), while the relative interaction parameters, like binding constants and thermodynamic parameters were given.

The gold nanoclusters (AuNCs) have attracted substantial research interest in the fields of chemistry [11, 12], materials [13, 14], biology [15-17], and medicine [18]. Considerable efforts have been devoted to exploring synthesis methods for stability, functionality and solubility of AuNCs [19-22]. The synthesis methods for AuNCs with biological macromolecules-mediated like DNA [23], peptide [24], bovine serum albumin (BSA) [25] and Pep [26] in the alkaline solution have been reported. In order to overcome the shortage of time-consuming for biosynthesized AuNCs, some technologies like microwave [27], photolithography [28] have gradually applied in bio-synthesize AuNCs. Photochemical induced effect (PCIE) as one of photo-induced effect [29, 30], it could not only quickly induce AuNCs generation in solution under biological macromolecules-mediated, but also endow AuNCs with some special photoelectric properties. In view of its special characterization,

the PCIE will open the new way for bio-synthesis AuNCs in solution. There is no report for on-line generated AuNCs in the flow inject-chemiluminescence (FI-CL) system and the application on the interaction of protein-drug.

Captopril (CAP, **Fig. 1**) has the significant antihypertensive effect as angiotensin converting enzyme inhibitors (ACEI), which could improve cardiac function in patients [31]. The methods for determining CAP in vivo are commonly considered as liquid chromatography-mass spectrometry (LC-MS) or liquid chromatography-column derivatization-UV detection (LC-CD-VWD) [32, 33]. But the time-consuming, expensive instrument and low sensitivity are the bottleneck of above methods for CAP determining in vivo. The CL methods have gradually become the general and practical methods for determining CAP with the high sensitivity and wide dynamic ranges [34]. Recently, Paraskevas has reviewed variety of flow related methods for CAP determination in both pharmaceutical and biological samples [35].

Fig. 1

It has been reported that $HAuCl_4$ as a co-reactant could remarkably increase the luminol CL intensity [36, 37]. Up to date, no flow inject-chemiluminescence (FI-CL) approach combined with $HAuCl_4$ and Pep has been designed and develped for drug analysis in vivo and Pep-drugs interaction. In this work, we developed an ingenious lumion-$HAuCl_4$-Pep FI-CL approach for CAP determining, and applied the proposed approach to study the CAP pharmacokinetics in rabbits with micro-dialysis. The aims of the present study were to: (1) investigate the mechanism of complex enhancement effect of CL and the complex quench effect of CL in luminol-$HAuCl_4$-Pep/CAP CL system (2) develop an ingenious luminol-$HAuCl_4$-Pep FI-CL approach to study CAP pharmacokinetic in rabbits with micro-dialysis.

Experimental Section

Chemical and reagents

All the reagents used were analytical grade. Water was purified by Milli-Q system (Millipore, Bedford, MA, USA) with the resistivity of 18.2 $M\Omega \cdot cm^{-1}$ and used throughout the whole experiment. Luminol (Fluka, Biochemika, Switzerland) and Pep (Procine gastric mucosa, 010M7006V, Sigma-Aldrich, St. Louis, MO, USA) were used without further purification. The CAP was purchased from the National institute of control of pharmaceutical and biological products, China. Chloroauric acid ($HAuCl_4$, analytical grade) was purchased from Shanghai reagent factory, China; Capoten Tablets (Sino-American Shanghai squib co., LTD, China, H20010430) were purchased from local dispensary.

Stock solution of CAP (1.0 $mmol \cdot L^{-1}$) and Pep (100.0 $\mu mol \cdot L^{-1}$) were prepared in purified water and stored at 4 °C. Working standard solutions of CAP and Pep were prepared daily by diluting the stock solution appropriately with purified water. Stock solution of luminol (2.5×10^{-2} $mol \cdot L^{-1}$) was prepared by dissolving 0.44 g luminol in 100 mL NaOH (1.0×10^{-1} $mol \cdot L^{-1}$) solution in a brown calibrated flask. Stock solution of $HAuCl_4$ (2.5×10^{-2} $mol \cdot L^{-1}$) was prepared by dissolving 1.0 g $HAuCl_4$ in 100 mL purified water and stored at 4 °C

Apparatus

The apparatus (Model IFFM-E, Xi'an Remax Electronic Science-Tech. Co. Ltd) of FI-CL system was consisted of the sampling system, the photomultiplier tube (PMT), and the PC with an

IFFM-E client system (Remax, Xi'an, China). Poly tetra fluoro ethylene (PTFE) tube (1.0 mm i.d.) was used to carry the solutions. The micro-dialysis system was composed of a CMA/100 microinjection pump, a CMA/140 micro-fraction injector (CMA, Stockholm, Sweden) and micro-dialysis probes (CMA/20, Beijing Ying Bo Li Da Technology Development Co., Ltd., China). The UV-Vis absorption spectra (225 ~ 800 nm) were collected using a U-3010 spectrophotometer system (Hitachi, Japan). The TEM images were obtained using a Tecnai G^2 F20 S-TWIJEM-2010 transmission electron microscope (FEI, USA) operated at 200 kV.

The profile for different systems with static injection CL

The static injection CL method was used to evaluate the CL kinetics progress for different CL systems. Using permutations way, four different FI-CL systems were designed to study the different CL mechanism. For the luminol-dissolved oxygen/CAP CL system, 100 μL luminol solution was directly injected into the dissolved oxygen solution at the absent or present of CAP. For luminol-$HAuCl_4$/CAP and luminol-Pep/CAP CL system, 100 μL luminol solution was injected into the $HAuCl_4$ solution and the Pep solution at the absent or present of CAP, respectively. For the luminol-$HAuCl_4$-Pep/CAP CL system, the Pep first mixed with CAP, then with $HAuCl_4$ to form the $HAuCl_4$-Pep/CAP solution at the present of CAP, finally 100 μL luminol solution was injected into above $HAuCl_4$-Pep/CAP solution. The CL intensity was collected by the PMT (negative voltage was set as 400 V) for 40 seconds.

The procedures of luminol-$HAuCl_4$-Pep CL combined with micro-dialysis

In the luminol-$HAuCl_4$-Pep CL system, five flow lines were inserted into the solutions of

luminol, carrier (purified water), $HAuCl_4$, Pep and CAP, respectively, and the solutions were propelled by peristaltic pumps. Luminol (100 μL) was quantitatively injected into the mixed solution of $HAuCl_4$, Pep and samples by six-way valve, then, the mixture was delivered into the flow cell producing CL emission which was detected by PMT (negative voltage was set as 700 V). The concentration of CAP was quantified by the decrement of CL intensity ($\Delta I = I_0 - I_s$), where I_s and I_0 were CL signals in the presence and in the absence of CAP samples, respectively.

A retrograde calibration technique was used for the assessment of in vivo recovery rate of the luminol-$HAuCl_4$-Pep CL system **(Fig. 2)**. Two hours post probe implantation, which served as a stabilization period, the perfuse (C_{perf}) and dialysate (C_{dial}) concentrations of CAP were determined by luminol-$HAuCl_4$-Pep FI-CL system. The relative loss of CAP during retro-dialysis L_{retro} or relative recovery (R_{dial}) by dialysis was then calculated as follow: $L_{retro} = R_{dial} = (C_{perf} - C_{dial})/C_{perf}$.

Fig. 2

Molecule docking

The MD of Pep-CAP was performed with the open-free soft of *Autodock* 4.2 using a semi-flexible docking mode. The crystal structure of Pep (PDB entry 1YX9) was obtained from the *Protein Data Bank*. The 3D structure of CAP were generated by the *ChemDraw* 10.0 and *Chem3D* 10.0 soft (Cambridge Soft, USA); and the energy-minimized conformation was obtained by the *Gasteiger-Huckel* Charges with a gradient of 0.005 kcal·molL^{-1} [38]. With the aid of *AutoDock* tools, the ligand root of CAP was detected and rotatable bonds were free-defined. The Grid box with 60 Å × 60 Å × 60 Å along x, y, z axes of 0.375 Å spacing was set in the whole process of MD. The population size and the maximum number of energy evaluation were set as 1.5×10^2 and 2.5×10^6,

155 respectively. The *Lamarckian Genetic Algorithm* was applied for docking simulations. The
156 conformation with the lowest binding energy was analyzed using *Pymol* 1.6.0.0.
157
158 **Method validation for CAP determining**
159 The proposed method was validated regarding its selectivity, linearity, the limit of detection
160 (LOD), accuracy, precision, recovery and stability. The linearity of methods were constructed
161 between the relative CL intensity and the different concentration of CAP. The LOD was considered
162 as the final concentration that produced a signal-to-noise (S/N) ratio of 3. The precision and
163 accuracy of the method were assessed by performing replicate analyses of CAP with anti-coagulant
164 citrate dextrose (ACD) solution consisting of citric acid 3.5×10^{-3} mol·L^{-1}, sodium citrate $7.5 \times$
165 10^{-3} mol·L^{-1}, and dextrose 13.6×10^{-3} mol·L^{-1}. The precision was determined from inter-day and
166 intra-day using six determinations of low, medium and high concentrations and expressed as
167 relative standard deviation (RSD%). The extraction recovery rate was determined by calculating the
168 ratio between the amounts of the drug-free samples and spiked with known amounts of CAP into
169 drug-free samples. The stability of the sample was assessed by measuring the analysis data of CAP
170 standard samples with high, medium and low concentration under ambient. To evaluate its
171 selectivity, the different foreign species were added to a standard solution of CAP, and assessed the
172 impact effect of foreign substances for standard CAP solution.
173
174 **The pharmacokinetic study of CAP in rabbits**
175 The Capoten Tablet was stripped of the outer sugar coating, grinded to powdery. The Capoten
176 Tablet powdery (1.00 g) was accurately weighted and placed in a beaker, added with 50 mL

177 deionized water with ultrasonic for 30 min, kept constant volume with purified water to 100 mL
178 brown volumetric flask, dark chilled.

179 Male rabbits (1.8 ~ 2.2 kg, n=5) were purchased from the Laboratory Animal Center of Xi'an
180 Jiaotong University (Xi'an, PR China) and housed in a cage with free access to food and water
181 available ad libitum. The animals were acclimated for at least one week with a 12 h light/dark cycle.
182 All experimental rabbit surgery procedures were approved by the institutional animal
183 experimentation committee of Xi'an Jiaotong University.

184 On the day of experiment, each rabbit was initially anesthetized with chloral hydrate solution
185 (1.0 $mg \cdot kg^{-1}$, subcutaneous) and catheters were positioned within the jugular vein toward the right
186 atrium and then perfused with ACD solution. The flow rate of ACD were set at 3.0 $\mu L \cdot min^{-1}$ by a
187 microinjection pump for blood micro-dialysis. The rabbit's body temperature was maintained at
188 37 °C with a heating blanket. Following 2 h stabilization period after surgery, CAP was
189 administrated with 1.16 $mg \cdot Kg^{-1}$ *via* intragastric (i.g.) administration. The dialysates were collected
190 every 25 min for 16 h and preserved at −4 °C refrigerator. The concentration of CAP in the
191 dialysate was determined by the luminol-$HAuCl_4$-Pep FI-CL system. CAP micro-dialysis
192 concentration (C_m) was converted to unbound concentration (C_u) as follows: $C_u = C_m / L_{retro}$.

193

194 **Result and discussion**

195

196 **Relative CL intensity-time profile**

197 The relative CL intensity-time profile of different photochemical reaction systems were
198 shown in **Fig. 3.** It could be seen from the CL intensity-time profile that the maximum time (T_{max})

for reaching maximum CL intensity (I_{max}) of luminol-dissolved oxygen and luminol-$HAuCl_4$ CL system (curve 2 and 6) was 3.0 s with the I_{max} of 45 and 550, respectively; compared with the luminol-dissolved oxygen and luminol-$HAuCl_4$ CL system, the T_{max} of luminol-Pep and luminol-$HAuCl_4$-Pep CL system (curve 4 and 8) were shortened from 3.0 s to 2.8 s, and the corresponding CL intensity for curve 4 and 8 were 104 and 1143, respectively. From this results, we could speculate that Pep could accelerate the electron transfer rate due to the proton process of luminol or luminol-$HAuCl_4$ and Pep in alkaline solution, which could lead to the shortage of T_{max} for curve 4 and 8. Compared with the CL system of curve 2 and 4, $HAuCl_4$ as the co-reactant could remarkably increase the luminol CL intensity. The reason might be attributed to the Au nuclei generated in the alkaline solution, which could cause the quantum confinement effect mediated by the PCIE of luminol. In the present of CAP (C_{CAP}=10.0 pmol·L^{-1}), it could sharply quench from 1143 to 1017 for luminol-$HAuCl_4$-Pep CL system with quenching ratio of 11.0%. For the CL system of luminol-dissolved oxygen, luminol-$HAuCl_4$ and luminol-Pep, almost had no or slightly inhibitory effect. This result could explain that luminol-$HAuCl_4$-Pep CL system had the higher sensitivity for the minor changes by the confirmation of Pep, which mediated by the interaction between Pep and CAP. Interesting, the CL intensity for curve 1-6 extinguished during 40 s, while the curve 7 and 8 had the higher stable CL intensity than other CL intensity and lasted for 80 s to extinguish.

Fig. 3

The CL intensity could be enhanced and inhibited while mixed alkaline luminol with different $HAuCl_4$-Pep solution and $HAuCl_4$-Pep/CAP solution. It could obtain the different CL response intensity (**Fig.3**). But for all of mentioned CL system, the luminol-$HAuCl_4$-Pep and

luminol-$HAuCl_4$-Pep/CAP CL intensity could be significantly enhanced and inhibited compared with other CL system. The mechanism of luminol-dissolved oxygen, luminol-Pep and luminol-$HAuCl_4$ have been explained in previous reports [39, 40]. Here we mainly focused on luminol-$HAuCl_4$-Pep and luminol-$HAuCl_4$-Pep/CAP CL system to explain the possible mechanism of AuNCs generated in alkaline solution and the interaction of Pep/CAP in the luminol-$HAuCl_4$-Pep CL system.

CL mechanism for luminol-$HAuCl_4$-Pep/CAP system

The complex enhancement effect of CL

To further confirm the above possible mechanism, the different reaction solution were investigated by TEM and UV-Vis absorption spectra under the fixed reactant concentration (**Fig. 4 and 5**). HR-TEM results showed sub-nanometer AuNCs could be generated in the luminol-$HAuCl_4$-Pep CL reaction solution with the average diameter distributed in 1-2 nm. The UV-Vis results showed the absorption wavelength of Pep was 256 nm, which smothering by the peak absorption of luminol; the characteristic absorption of luminol had the decreasing tendency at the 285 nm and 325 nm; meanwhile, a new absorption peak at 545 nm was produced, which is Au atom character absorption peak [41]. Based on this characterization, we could make the conclusion that $HAuCl_4$ firstly formed Pep-Au (III) complex in CL system, then reduced to Au atom and eventually formed the sub-nanometer AuNCs by luminol photochemical induced effect [42, 43], while injected into the alkaline luminol solution with the flow rate of 2.0 $mL \cdot mol^{-1}$.

Fig. 4

Fig. 5

Combined with the results of TEM and UV-Vis, in the profile of luminol-$HAuCl_4$-Pep CL system, it was found that Pep-Au (III) complex was firstly formed while mixed Pep with $HAuCl_4$; then was reduced while added into alkaline luminol solution (**Fig. 6**). The detailed mechanism could refer to our previous report about photochemical induced formed Au nanomaterial with size and shape controlled by luminol-Pep CL reaction [44]. The AuNCs generated in the luminol-$HAuCl_4$-Pep CL system was conducted at the fixed alkaline luminol solution with the pH value of 10.5. From the perspective of the experimental performance, the alkaline luminol had the optimal luminous efficiency at the pH of 10.5, which could improve the detection sensitivity. Due to the properties of sub-nanometer size and good hydrophilic, AuNCs could effectively prevent pipeline blockage, which caused by the effect of deposition and aggregation of the AuNCs, to disturb the sensitivity and reproducibility for CAP determining.

Fig. 6

The complex quench effect of CL

Using the established model of protein-small molecule interaction [45], the corresponding binding parameters for CAP to Pep, K and n, were 1.7×10^6 L·mol^{-1} and 0.87, respectively. The results showed that the 1:1 Pep/CAP complex was formed. The thermodynamic parameters of CAP to Pep were calculated using the *Van't Hoff* equation [46]. The results indicated that the $\Delta H^o > 0$, $\Delta S^o > 0$ and $\Delta G^o < 0$ at different temperatures **(Table 1)**. It could deduce that the binding force was mainly on the hydrophobic interaction [47]. The MD studies could give some insight into the protein-drug interactions [48, 49]. In the presence of CAP, the docked conformation of Pep/CAP was

shown in **Fig. 7**. The docked pose showed that CAP might enter into the active site cavity of Pep and form the hydrogen bind to ASP32 with the bind distance of 3.2 Å. For Pep/CAP complex, the inhibition constants, free energy of binding and accessible surface area (ASA) were 8.7×10^5 $L \cdot mol^{-1}$, -30.44 $kJ \cdot mol^{-1}$ and 119.38 $Å^2$, respectively (**Table 2**).

Table 1

Table 2

Fig. 7

In the luminol-$HAuCl_4$-Pep/CAP CL system, CAP solution first mixed with Pep solution under neutral conditions, and then mixed successively with $HAuCl_4$ solution, alkaline luminol solution (pH = 10.5). In the profile of luminol-$HAuCl_4$-Pep/CAP CL system, it was found that the CL intensity of luminol-$HAuCl_4$-Pep/CAP could effectively inhibited compared with the CL intensity of luminol-$HAuCl_4$-Pep. The reason might be attributed to the interaction of Pep-CAP. For Pep conformation, the Asp32 as negative charge polar residue locate on the interface cleft of Pep [50]. For the structure of CAP, the thiol group (-SH) and carboxyl group (-COOH) made it easily to form the hydrophilic microenvironment due to the strong electron-withdrawing effect. In Pep/CAP complex **(Fig. 7)**, the O atom of carbonyl group in CAP could bind to the Asp32 of Pep with hydrogen bond and enter into hydrophilic center of Pep, which is formed by the two activity sites, Asp32 and Asp 215 on the each cleft of Pep. The interaction of Asp32 and carbonyl group had the ability of accessibly to be protonated between Pep and CAP. The thiol group of CAP as the special group play the key function for drug-efficacy in vivo. The thiol group in the Pep/CAP complex had no binding with other group of Pep. This results indicated that the bio-activity of CAP was not

287 influenced by the activity center of Pep, while in the process of protein-drug interaction between
288 Pep and CAP. The flexible loop formed with Asp32 and Asp215, which is commonly known as the
289 "flap", could induce the conformation change of Pep [51]. With the Pep-CAP interaction, the amino
290 acid residues on the Pep surface like Asp11, Asp159, Glu4, Glu13 and Asp118 would be embedded
291 into the internal of Pep. The abnormally high p*Ka* values of Asp11 and Asp159 gradually trended
292 to normal value due to the protonated process between Pep and CAP. This change would directly
293 promote reduction potential reduce, which could inhibit Au atom aggregation on the surface of Pep
294 with other amino acid residues, produce the CL quenching effect.

295 In short, the possible mechanism for producing sub-nanometer AuNCs, enhancing the CL
296 intensity and inhibiting the CL intensity while added CAP might be as follows:

297 (1) Under the alkaline condition, Au^{3+} and negatively charge amino acid residues could form
298 the Pep-Au^{3+} complex on the surface of Pep. Due to the instability conformation of Pep at the
299 alkaline solution, the negative charged polar residue with abnormally high pKa values could
300 promote the Au^{3+} flowing into the vicinity of negatively charged amino acid residues on the
301 principle of charge density matching and form sub-nanometer AuNCs [52], Meanwhile, microscopic
302 changes of Pep confirmation could accelerate the electrons transferring rate of excited
303 3-aminophthalate, giving the enhancement CL intensity of luminol and producing complex
304 enhancement effect of CL (CEC).

305 (2) CAP could bind to Asp32 with hydrogen bond, and enter into hydrophilic center of Pep,
306 lead to Pep's conformation change, reduce the reduction potential on the Pep's surface. Based on
307 the cascading effect of Pep/CAP interaction, the electrons transferring rate of excited
308 3-aminophthalate was inhibited, and produced the complex quench effect of CL (CQC)

CL experimental conditions

In order to obtain the optimum performance for developing the luminol-$HAuCl_4$-Pep FI-CL approach, the concentration of luminol, NaOH, $HAuCl_4$, Pep, the flow rate and mixing tube length were systematically optimized for the whole experiment **(Table 3)**. The effects of luminol concentration from 5.0×10^{-7} to 2.5×10^{-4} mol·L^{-1} were tested. It was found that with the increasing of luminol concentration, the CL signal increased steadily until luminol of 2.5×10^{-4} mol·L^{-1}, and tended to be stable, thus 2.5×10^{-4} mol·L^{-1} was chosen as the optimum luminol concentration. Due to the alkaline medium-dependent nature of the luminol CL reaction [54], NaOH solution with concentrations ranging from 5.0×10^{-3} to 2.0×10^{-1} mol·L^{-1} were tested. It was found that NaOH had the ability to increase the sensitivity of CL system; 2.5×10^{-2} mol·L^{-1} NaOH was finally chosen as the optimum concentration. Pep had a linear relationship for enhancing the luminol CL intensity from 1.0×10^{-10} mol·L^{-1} to 1.0×10^{-6} mol·L^{-1}. Based on the fundament of luminol-Pep CL response, $HAuCl_4$ could sharply increase the luminol-Pep CL signal in the range of $1.0 \times 10^{-6} \sim 1.5 \times 10^{-4}$ mol·L^{-1}. In the luminol-$HAuCl_4$-Pep CL system. The concentration of Pep and $HAuCl_4$ were finally set as 1.0×10^{-6} mol·L^{-1} and 2.5×10^{-5} mol·L^{-1}, respectively, for the consideration of the whole system of sensitivity, background noisy and possible pipes clogging effect of AuNCs. Meanwhile, the flow rate of the system was the key factor for obtaining the good sensitivity, signal-to-noise, and prevent the CL spectrum broadening, the flow rate was set 2.0 mL·min^{-1}. The mixing tube was set 10.0 cm for good sensitivity and reproducibility.

Table 3

In vivo recovery of CAP from micro-dialysis probe

Micro-dialysis as one of micro-flow system has been successfully used for continuous in vivo sampling in biomedical, pharmacological and neuroscience studies [55, 55]. In the process of samples collection, the flow rate was the key factor for the dialysis recovery ratio. Here, in order to obtain better micro-dialysis recovery ratio, different flow rate of dialysate were studied under the fixed CAP concentration (210.0 $pg \cdot mL^{-1}$). The results showed in **Fig. 8**, the recovery ratio largely decreased from 53% to 38.9%, while the flow rate increasing from 0.05 to 3.0 $\mu L \cdot min^{-1}$. After 3.0 $\mu L \cdot min^{-1}$, the recovery ratio reached near-steady-state period. The reason for this result would be that, at the low flow rate, the concentration was the key factor; while for high flow rate, it was mainly controlled by size of porous membrane [56]. Comprehensive consideration of various factors, like recovery ratio, dialysis pressure, cut-off ratio and membrane permeation, the flow rate was eventually set as 3.0 $\mu L \cdot min^{-1}$ for the whole micro-dialysis experiment.

Fig. 8

It is well known that the efficiency of micro-dialysis was mainly controlled by some distinct factors, which included surface area of the dialysis membrane, molecule cut-off rate and the CAP concentration. The length of blood probe membrane was 2.5 cm and the molecule weight of CAP was 217.29, which was much less than the maximum cut-off limitation (3.5 kD). To evaluate the in vivo recovery, the micro-dialysis probe was located in the three unknown concentration of CAP blood (CAP standard solution + blank serum) (2.1, 21.0, 210.0 and 2100.0 $pg \cdot mL^{-1}$) with 3.0 $\mu L \cdot min^{-1}$ of ACD solution for micro-dialysis to determining the factual CAP concentration according to the linear relationship of luminol-$HAuCl_4$-Pep CL system. The results of average recoveries of three different CAP concentration were 36.8 ± 0.02, 38.9 ± 0.05, 41.2 ± 0.08 and 42.8

± 0.13% in blood, respectively. The data indicated that the recovery for micro-dialysis probes in blood shared no significant differences among the concentration ranges of 2.1, 21.0, 210.0 and 2100.0 $pg \cdot mL^{-1}$. These results suggested that the recovery for micro-dialysis probes was concentration independent, which could be applied to study of CAP pharmacokinetic in rabbits.

Method validation

Linearity and LOD

A series of CAP standard solutions were injected into the manifold depicted in above mentioned **Fig. 2** with the different CL system of luminol-dissolved oxygen, luminol-$HAuCl_4$, luminol-Pep and luminol-$HAuCl_4$-Pep. The decrement of the CL was proportional with the concentration of CAP, and the correspondent linear equation and limit of detection (LOD) were listed in the **Table 4**. Compared with luminol-dissolved oxygen and luminol-$HAuCl_4$ system, luminol-Pep CL system had the good sensitivity of 2.3 $pmol \cdot L^{-1}$ for CAP. Apparently, luminol-$HAuCl_4$-Pep CL system had the wide linear range and good sensitivity for CAP determining from 3.0 $pmol \cdot L^{-1}$ to 0.1 $\mu mol \cdot L^{-1}$, with LOD of 1.0 $pmol \cdot L^{-1}$.

Table 4

Stability, precision and accuracy

The operational stability were tested for 210.0, 21.0 and 2.1 $pg \cdot mL^{-1}$ in the correspondent FI-CL system, and the relative CL intensity ($\Delta I = I_s - I_0$) were recorded. The experiments were performed for 5 days with the FI-CL system regularly used over 8 h per day and the results were

listed in **Table 5.** It was found that ΔI kept stable under the fluctuation of I_0 and the RSD were less than 5.0 % with satisfying stability of the correspondent FI-CL system. At a flow rate of 2.0 $mL \cdot min^{-1}$, a complete determination of CAP, including sampling and washing, could be accomplished in 0.5 min, given a throughout of 120 h^{-1} with a RSD of less than 5.0 %. Inter-day and intra-day precision and accuracy data were shown in Table 6. The RSD of inter-day and intra-day precision for different CAP concentration were less than 4.78, and the recovery rate for different concentration of CAP in ACD solution and blank dialysis were more than 95.42%, indicated the overall reproducibility, precision and accuracy of the proposed method.

Table 5

Table 6

Interference studies

The interferences of foreign species were tested by analyzing a standard solution of CAP into which increasing amounts of potential interfering substances were added. The tolerable concentrations of foreign species with respect to 50 $nmol \cdot L^{-1}$ CAP for interference at 5.0% level were less than 100 $\mu mol \cdot L^{-1}$ for methanol and ethanol; 5.0 $\mu mol \cdot L^{-1}$ for I^-, SO_4^{2-}, PO_4^{3-}, BrO_3^-, glucose and citric acid; 3.0 $\mu mol \cdot L^{-1}$ for Mg^{2+}, Ca^{2+}, Zn^{2+} and Ba^{2+}; and Fe^{3+}/Fe^{2+}; 160 $\mu mol \cdot L^{-1}$ for chloral hydrate, respectively.

In order to eliminate disturbance of dialysate and improve the sensitivity of determining CAP in rabbit's blood dialysate, the interference of blank blood dialysate were tested by diluting serials blank blood dialysate with purified water to gain similar to the same of the luminol-$HAuCl_4$-Pep CL intensity. In the presence of blank blood dialysate, the relative CL intensity in the system of

luminol-$HAuCl_4$-Pep was approximately equal to the CL intensity in the absence of blank blood while diluted 5×10^3 times with purified water.

The pharmacokinetics of CAP in blood

Following the above method described, an aliquot (20 μL) of rabbit blood dialysate was determined after appropriate dilution (dilution factor = 5×10^3), the results were listed in **Table 7**. It could be seen that the recoveries ratio from 89.0 % to 112 % with RSDs less than 5.0 %. The CAP concentration-time fitting curves for 5 rabbits after i.g. administration were shown as **Fig. 9**.

Fig. 9

Table 7

The pharmacokinetic parameters for CAP in dialysate were obtained with the aid of the *DAS* soft. Various parameters such as area under curve (*AUC*), peak plasma concentration (C_{max}), time to reach the peak (T_{max}), and elimination rate constant (K_{el}), absorption and elimination half-life ($T_{1/2}$), the total mean residence time (*MRT*) and absorption efficiency were calculated for each rabbit. $AUC_{0-\infty}$ was calculated as $AUC_{0-t} + C_{last}/K_{el}$, where C_{last} is the last measurable concentration. The volume of distribution was obtained as dose/$AUC_{0-\infty}$. The mean pharmacokinetic parameters for 5 rabbits were list in **Table 8**. The results showed that the maximum peak concentration of CAP was 9.63 ± 1.45 μg·mL^{-1} at 0.75 ± 0.08 h and the detectable quantity (6.23 ± 0.4 pg·mL^{-1}) was found at 16 h after its i.g. administration, which was higher than the limit of quantity (LOQ) of the analytical approach. Meanwhile, the value of higher AUC_{0-t} (613.16 ± 5.09 mg·L^{-1}·h^{-1}), *V1/F* (2.02 ± 0.17 L·g^{-1}) and lower MRT_{0-t} time (12.47 ± 0.39 h) showed that CAP had the stronger ability of penetrating of biological membranes and mainly distributed in the richen blood of organ and tissue

in vivo, excreted with the prototype with *CL/F* (7.27 ± 0.41 $L \cdot g^{-1} \cdot h^{-1}$). After a single i.g. of CAP, it could rapidly absorbed from the gastro-intestinal tract with peak blood level of 0.8 $\mu g \cdot mL^{-1}$ in about an hour period with the minimal absorption of 75%. Up to 50% of CAP was metabolized through the liver, oxidized to their respective disulfides, and the remaining was excreted in the urine [58, 59]. The results showed that CAP could be in line with the two-compartment open model in vivo.

Table 8

The statistical analysis of main pharmacokinetic parameters, such as $AUC_{0\text{-t}}$, *V1/F*, $MRT_{0\text{-t}}$, *CL/F* and C_{max} were performed using the one-way analysis of variance (ANOVA) followed by Spss19.0 soft. The statistical results showed that the pharmacokinetic parameters had no significant specific difference ($P > 0.05$).

Conclusion

Based on the luminol CL intensity enhanced by Pep and $HAuCl_4$, an ingenious luminol-$HAuCl_4$-Pep FI-CL system was constructed for the first time. In the proposed FI-CL system, the sub-nanometer AuNCs was generated in the luminol-$HAuCl_4$-Pep CL reaction solution, which could potentially enhance the CL intensity; the possible mechanism for enhancing the CL intensity with $HAuCl_4$ and Pep was given. This proposed FI-CL approach was successfully applied to study the CAP pharmacokinetic in rabbit with micro-dialysis. The results showed that CAP have the C_{max} (9.63 ± 1.45 $\mu g \cdot mL^{-1}$) at T_{max} (0.75 ± 0.08 h), corresponding with $t_{1/2\beta}$ (3.19 ± 0.13 h) and CL/F (7.27 ± 0.41 $L \cdot g^{-1} \cdot h^{-1}$) in rabbits vivo. The pharmacokinetic results showed the CAP fit two-compartment open model in rabbits.

Acknowledgments

This work was supported by the National Natural Science Foundation of China (No. 21275118) and the Open Fund from Key Laboratory of Synthetic and Natural Functional Molecule Chemistry of Ministry of Education.

References

[1] J.P. Renaud and M.A. Delsuc, Curr. Opin. Pharmacol., 2009, 9, 622-628.

[2] W.F.J. de Azevedo, R.A. Caceres, I. Pauli, L.F. Timmers, G.B. Barcellos, K.B. Rocha and M.B. Soares, Curr. Drug Targets, 2009, 10, 271-278.

[3] S.M. Huang, H. Zhao, J.I. Lee, K. Reynolds, L. Zhang, R. Temple and L.J. Lesko, Clin. Pharmacol. Ther., 2010, 87, 497-503.

[4] R. Minai, Y. Matsuo, H. Onuki and H. Hirota, Proteins, 2008, 72, 367-381.

[5] J. Colinge, U. Rix, K.L. Bennett and G. Superti-Furga, Proteomic, 2012, 6, 102-116.

[6] B.M. Dunn, Chem. Rev., 102 (2002) 4431-4458.

[7] D.R. Dee and R.Y. Yada, Biochemistry, 2010, 49, 365-371.

[8] H.M. Zhang, J. Cao, Z.H. Fei and Y.Q. Wang, J. Mol. Struct., 2012, 1021, 34-39.

[9] H.J. Zeng, T.T. Qi, R. Yang, J. You and L.B. Qu, J. Fluoresc., 2014, 24, 1031-1040.

[10] S.Q. Lian, G.R. Wang, L.P. Zhou and D.Z. Yang, Luminescence, 2013, 28, 967-972.

[11] H.J. Zhang, T. Watanabe, M. Okumura, M. Haruta and N. Toshima, Nat. Mater., 2011, 11, 49-52.

[12] H. Häkkinen, S. Abbet, A. Sanchez, U. Heiz and U. Landman, Angew. Chem. Int. Edit., 2003, 42, 1297-1300.

463 [13] W. Chen and S.W. Chen, Angew. Chem. Int. Edit., 2009, 48, 4386-4389.

464 [14] Z.W. Wang and R.E. Palmer, Nano Lett., 2011, 12, 91-95.

465 [15] C.A.J. Lin, T.Y. Yang, C.H. Lee, S.H. Huang, R.A. Sperling, M. Zanella, J.K. Li, J.L. Shen,

466 H.H. Wang, and H.I. Yeh, ACS Nano, 2009, 3, 395-401.

467 [16] S. Palmal and N.R. Jana, Wires. Nanomed. Nanobi., 2013 DOI: 10.1002/wnan.1245

468 [17] H.H. Wang, C.A.J. Lin, C.H. Lee, Y.C. Lin, Y.M. Tseng, C.L. Hsieh, C.H. Chen, C.H. Tsai, C.T.

469 Hsieh and J.L. Shen, ACS Nano, 2011, 5, 4337-4344.

470 [18] W.Y. Chen, J.Y. Lin, W.J. Chen, L.Y. Luo, D.E. Wei-Guang and Y.C. Chen, Nanomedicine,

471 2010, 5, 755-764.

472 [19] Z.K. Wu, M.A. MacDonald, J. Chen, P. Zhang and R.C. Jin, J. Am. Chem. Soc., 2011, 133,

473 9670-9673.

474 [20] C.L. Liu, H.T. Wu, Y.H. Hsiao, C.W. Lai, C.W. Shih, Y.K. Peng, K.C. Tang, H.W. Chang, Y.C.

475 Chien and J.K. Hsiao, Angew. Chem. Int. Edit., 2011, 50, 7056-7060.

476 [21] R.C. Jin, H.F. Qian, Z.K. Wu, Y. Zhu, M.Z. Zhu, A. Mohanty and N. Garg, J. Phys. Chem.

477 Lett., 2010, 1, 2903-2910.

478 [22] Z.K. Wu and R.C. Jin, Nano Lett., 2010, 10, 2568-2573.

479 [23] G.Y. Liu, Y. Shao, K. Ma, Q.H. Cui, F. Wu and S.J. Xu, Gold Bull., 2012, 45, 69-74.

480 [24] J. George and K.G. Thomas, J. Am. Chem. Soc., 2010, 132, 2502-2503.

481 [25] J.P. Xie, Y.G. Zheng and J.Y. Ying, J. Am. Chem. Soc., 2009, 131, 888-889.

482 [26] H. Kawasaki, K. Hamaguchi, I. Osaka and R. Arakawa, Adv. Funct. Mater., 2011, 21,

483 3508-3515.

484 [27] L. Yan, Y.Q. Cai, B.Z. Zheng, H.Y. Yuan, Y. Guo, D. Xiao and M.M.F. Choi, J. Mater. Chem.,

2012, 22, 1000-1005.

[28] H. Yabu, Chem. Commun., 2011, 47, 1196-1197.

[29] S.H. Lee, A.G. Larsen, K. Ohkubo, Z.L. Cai, J.R. Reimers, S. Fukuzumi and M.J. Crossley, Chem. Sci., 2012, 3, 257-269.

[30] H. Zeng, X.W. Du, S.C. Singh, S.A. Kulinich, S. Yang, J. He, and W. Cai, *Adv. Funct.Mater.*,

[31] R.F. Popovici, E.M. Seftel, G.D. Mihai, E. Popovici and V.A. Voicu, J. Pharm. Sci., 2011, 100, 704-714.

[32] W.M.M. Mahmoud and K. Kümmerer, Chemosphere, 2012, 88, 1170-1177.

[33] N. Rastkari, M. Khoobi, A. Shafiee, M.R. Khoshay and R. Ahmadkhaniha, J. Chromatogr. B, 2013, 932, 144-151.

[34] P. Khan, D. Idress, M.A. Moxley, J.A. Corbett, F. Ahmad, G.V. Figura, W.S. Sly, A. Waheed and M.I. Hassan, Appl. Biochem. Biotechnol., 2014, 173, 333-355.

[35] P.D. Tzanavaras, Anal. Lett., 2011, 44, 560-576.

[36] M. Iranifam, TrAC Trend Anal. Chem., 2013, 51, 51-70.

[37] Q.Q. Li, L.J. Zhang, J.G. Li and C. Lu, TrAC Trend Anal. Chem., 2011, 30, 401-413.

[38] J. Wang, S.H. Zhang, J. Zhang, P. Ren, Y.C. Chen, J.H. Li, W. Wang, Y. Ma, R.F. Shi and C.H. Wang, J. Chromatogr. B, 2011, 879, 1605-1609.

[39] X.J. Tan, Z.M. Wang, D.H. Chen, K. Luo, X.Y. Xiong and Z.H. Song, Chemosphere, 2014, 108, 26-32

[40] Z.F. Zhang, H. Cui, C.Z. Lai and L.J. Liu, Anal. Chem., 2005, 77, 3324-3329.

[41] Z. Wu, M.A. MacDonald, J. Chen, P. Zhang and R. Jin, J. Am. Chem. Soc., 2011, 133, 9670-9673.

[42] Y.S. Chen and P.V. Kamat, J. Am. Chem. Soc., 2014, DOI: 10.1021/ja501736.

[43] T.P. Yoon, M.A. Ischay and J. Du, Nat. Chem., 2010, 2, 527-532.

[44] K. Luo, X.H. Zheng, Z.H. Song, RSC Adv. 2014, DOI: 10.1039/C4RA07283A

[45] Z.M. Wang and Z.H. Song, Analyst, 135 (2010) 2546-2553.

[46] O. Cañadas and C. Casals, Methods Mol. Biol., 2013, 974, 55-71.

[47] X.Y. Gao, Y.C. Tang, W.Q. Rong, X.P. Zhang, W.J. Zhao and Y.Q. Zi, Am. J. Anal. Chem., 2011, 2, 250-257.

[48] Y. Chen And B.K. Shoichet, Nat. Chem. Biol., 2009, 5, 358-364.

[49] A.S. El-Azab, M.A. Al-Omar, A.A.M. Abdel-Aziz, N.I. Abdel-Aziz, M.A.A. El-Sayed, A.M. Aleisa, M.M. Sayed-Ahmed and S.G. Abdel-Hamide, Eur. J. Med. Chem., 2010, 45, 4188-4198.

[50] D. Dee, J. Pencer, M.P. Nieh, S. Krueger, J. Katsaras and R.Y. Yada, Biochemistry, 2006, 45, 13982-13992.

[51] J.R. Engen, Anal. Chem., 2009, 81, 7870-7875.

[52] J.W. Liu, TrAC Trend Anal. Chem., 2014, DOI:10.1016/j.trac.2013.12.014

[54] H. Albrecht, Phys. Chem. Chem. Phys., 1928, 136, 321-330.

[55] P. Nandi and S.M. Lunte, Anal. Chim. Acta, 2009, 651, 1-14.

[56] H. Ronald Zielke, C.L. Zielke and P.J. Baab, J. Neurochem., 2009, 109, 24-29.

[57] D. Feuerstein, A. Manning, P. Hashemi, R. Bhatia, M. Fabricius, C. Tolias, C. Pahl, M. Ervine, A.J. Strong and M.G. Boutelle, J. Cerebr. Blood F. Met., 2010, 30, 1343-1355.

[58] A. Luczak, R. Zakrzewski and M. Dobrogowski, Bioanalysis, 2012, 4, 1481-1489.

[59] G. Donáth-Nagy, S.Vancea and S. Imre, Croa. Chem. Acta, 2011, 84, 423-427.

Captions for Figures

Fig.1. The structure of CAP

Fig.2. The scheme of CAP determination in rabbit blood of luminol-$HAuCl_4$-Pep FI-CL system with micro-dialysis

Fig.3. The kinetic curve for different CL reaction.

Curve 1: luminol-dissovled oxygen-CAP (C_{CAP} = 5.0 nM); Curve 2: luminol-dissolved oxygen; Curve 3: luminol-Pep-CAP (C_{CAP} = 7.0 pM); Curve 4: luminol-Pep; Curve5: luminol-$HAuCl_4$-CAP (C_{CAP} = 30.0 pM); Curve 6: luminol-$HAuCl_4$. Curve 7: luminol-$HAuCl_4$-Pep-CAP (C_{CAP} = 10.0 pM); Curve 8: luminol-$HAuCl_4$ -Pep.

The corresponding concentrations of luminol, $HAuCl_4$ and Pep were 2.5×10^{-4}, 2.5×10^{-5} and 1.0×10^{-6} mol·L^{-1}, respectively.

Fig.4. HR-TEM images of sub-namometers particles AuNCs generated in the luminol-$HAuCl_4$-pepsin CL reaction solution

Fig.5. The UV-Vis graphic of luminol-$HAuCl_4$-Pep system with the pH of 10.5. The corresponding concentrations of luminol, $HAuCl_4$ and Pep were 2.5×10^{-4}, 2.5×10^{-5} and 1.0×10^{-6} mol·L^{-1}, respectively.

Fig.6. Schematic illustration of the CL enhancement and AuNCs generation mechanism in luminol-$HAuCl_4$-Pep CL reaction

Fig.7. The structure of CAP binding to Pep.

Fig.8. The relationship curve between flow rate and recovery ratio for fixed concentration of CAP (210.0 pg·mL^{-1}) in the micro-dialysis system.

Fig.9. The CAP concentration-time fitting curves for 5 rabbits after intragastric (i.g.) administration

Table 1.The thermodynamic parameters of Pep-CAP

Tem. K	K $L \cdot mol^{-1}$	n	ΔH $kJ \cdot mol^{-1}$	ΔS $J \cdot mol^{-1} \cdot K^{-1}$	ΔG $kJ \cdot mol^{-1}$
283	8.1×10^5	0.67			−32.03
288	9.8×10^5	0.75			−33.02
293	1.3×10^6	0.84	24.48	199.68	−34.03
298	1.7×10^6	0.87			−35.02
313	2.2×10^6	0.89			−38.02

Table.2 The binding results of CAP to Pep by FI-CL model and molecule docking

FI−CL		Molecule docking	
n	0.87	Binding site(n)	Asp32
K_E ($L \cdot mol^{-1}$)	1.7×10^6	Bind distance (Å)	3.2
ΔH^o ($kJ \cdot mol^{-1}$)	24.48	K_M ($L \cdot mol^{-1}$)	8.7×10^5
ΔS^o ($kJ \cdot mol^{-1} \cdot K^{-1}$)	199.68	ASA($Å^2$)	119.38
ΔG^o (298.13 K)($kJ \cdot mol^{-1}$)	−35.03	ΔG^o (298.13 K) ($kJ \cdot mol^{-1}$)	−30.44

Table 3. The optimum performance of luminol-$HAuCl_4$-Pep FI-CL system

Optimum factors	Optimum range	Finial setting
luminol	$5.0 \times 10^{-7} \sim 2.5 \times 10^{-4}$ mol·L^{-1}	2.5×10^{-4} mol·L^{-1}
NaOH	$5.0 \times 10^{-3} \sim 2.0 \times 10^{-1}$ mol·L^{-1}	2.5×10^{-2} mol·L^{-1}
$HAuCl_4$	$1.0 \times 10^{-6} \sim 1.5 \times 10^{-4}$ mol·L^{-1}	2.5×10^{-5} mol·L^{-1}
Pep	$1.0 \times 10^{-10} \sim 1.0 \times 10^{-6}$ mol·L^{-1}	1.0×10^{-6} mol·L^{-1}
flow rate	1.0 ~ 5.0 mL·min^{-1}	2.0 ml·min^{-1}
mixing tube	5-20 cm	10 cm

Table 4. The linear and LOD for CAP in different luminol FI-CL system

FI-CL	Linear equation	Linear range	LOD	R^2
dissolved oxygen	ΔI = 11.205lnC + 60.96	10.0 nM-30 μM	3.0 nM	0.998
Pep	ΔI = 35.40lnC + 948.5	7.0 pM-3.0 nM	2.3 pM	0.983
$HAuCl_4$	ΔI = 53.08lnC + 1445.2	30.0 pM-100.0 nM	10.0 pM	0.988
$HAuCl_4$-Pep	ΔI = 125.63lnC + 3310.2	3.0 pM-0.1 μM	1.0 pM	0.995

594

595

596

597

Table 5. The stability of FI-CL system under different concentration of CAP

Time day	I_o	RSD %	I_s(2.1) pg·mL^{-1}	RSD %	I_s (21.0) pg·mL^{-1}	RSD %	I_s (210.0) pg·mL^{-1}	RSD %
1st	1132	1.5	1004	1.6	715	2.6	426	3.8
2nd	1125	1.8	997	2.3	708	3.1	419	3.5
3rd	1122	1.9	994	2.6	705	3.2	416	4.1
4th	1135	2.1	1007	2.3	718	2.3	429	4.3
5th	1130	2.3	1002	2.0	713	2.5	424	4.6

598

599

600

Table 6. The precision and accuracy of the proposed method

QC Sampl	Precision (n=5)		ACD solution(n=5)		Blank dialysis (n=5)	
$pg \cdot mL^{-1}$	Inter-day	Intra-day	Found	Recovery	Found	Recovery
2.10	2.08 ± 0.12	2.06 ± 0.22	2.08 ± 0.12	99.04%	2.02 ± 0.19	96.19%
21.0	20.32 ± 1.69	20.09 ± 2.89	20.32 ± 1.69	96.76%	20.04 ± 1.95	95.42%
210.0	202.87 ± 3.89	196.87 ± 4.78	202.87 ± 3.89	96.60%	200.96 ± 4.61	95.69%

601

602

603

604

605

606

607

608

609

610

611

612

613

614

615

Table 7. Determination of CAP in rabbit blood for 16 h [a]

Interval h	Added/found pg·mL^{-1}	RSD %	Recovery %	Content ng·mL^{-1}	Eliminate %
0.00	0/–	–	99.3	–	–
	2.10/2.02	0.5			
0.08	0/3.15	0.9	98.28	18.53 ± 0.83	0.01
	21.00/24.09	0.6			
0.16	0/28.51	2.8	106.43	40.07 ± 0.84	0.19
	21.0/51.34	1.2			
0.25	0/78.42	2.3	118.43	59.51 ± 0.79	0.38
	210.0/302.87	1.2			
0.50	0/172.55	1.8	96.29	171.22 ±0.72	0.89
	210.0/376.15	1.8			
0.75	0/151.84	2.7	107.38	411.55 ± 0.53	1.87
	210.0/373.05	1.9			
1.00	0/129.7	1.9	99.44	1003.59 ± 0.47	8.02
	210.0/339.00	3.2			
1.50	0/103.12	1.6	105.17	1595.53 ± 0.09	12.93
	210.0/318.45	2.5			
2.00	0/83.39	1.9	104.44	1277.57 ± 0.14	9.14
	210.0/297.09	3.3			
3.00	0/57.83	1.6	100.10	942.46 ± 0.29	4.38
	210.0/267.89	4.1			
4.00	0/36.26	2.8	109.09	661.09 ± 0.35	3.12
	21.0/60.56	3.7			
5.00	0/23.58	2.6	109.57	460.35 ± 0.39	2.26
	21.0/46.84	3.4			
6.00	0/7.20	2.9	115.82	320.30 ± 0.44	1.42
	2.1/10.44	4.6			
8.00	0/3.97	4.1	107.17	155.87 ± 0.58	0.73
	2.1/6.35	4.2			
10.00	0/1.16	3.5	113.97	75.18 ± 0.63	0.45
	2.1/3.42	3.2			
12.00	0/0.63	2.8	95.14	36.45 ± 0.87	0.26
	2.1/2.70	4.0			
14.00	0/0.44	3.5	98.53	18.54 ± 0.89	0.14
	2.1/2.53	4.3			
16.00	0/0.31	3.6	100.38	8.15 ± 1.02	0.05
	2.1/2.41	2.8			
Total eliminate rate					45.9

[a] 2.32 mg CAP was i.g. administration for rabbit (2.0 kg).

616

617

618

Table 8. The pharmacokinetic parameters of CAP in rabbits after intragastric (i.g.) administration (n=6)

Parameters	Samples No.					
	1#	2#	3#	4#	5#	M ± SD
$t_{1/2\alpha}$ (h)	0.187	0.203	0.219	0.196	0.256	0.212 ± 0.07
$t_{1/2\beta}$ (h)	3.56	3.17	3.24	2.88	3.11	3.192 ± 0.13
V1/F ($L \cdot g^{-1}$)	3.24	2.84	3.02	3.15	2.87	2.02 ± 0.17
CL/F ($L \cdot g^{-1} \cdot h^{-1}$)	8.12	7.01	6.35	7.24	7.63	7.27 ± 0.41
AUC_{0-t} ($mg \cdot L^{-1} \cdot h^{-1}$)	569.42	486.13	721.36	688.29	600.58	613.16 ± 5.09
T_{max} (h)	0.79	0.72	0.76	0.75	0.71	0.75 ± 0.08
C_{max} ($\mu g \cdot mL^{-1}$)	7.34	8.18	9.24	11.36	11.02	9.63 ± 1.45
MRT_{0-t} (h)	12.36	11.45	13.27	12.22	13.06	12.47 ± 0.39

AUC_{0-t}, under the curve up to the last time (t); T_{max}, the time to reach peak concentration; C_{max}, the maximum plasma concentration; V1/F, the apparent volume of distribution; K, the apparent rate constant; $t_{1/2\alpha}$ and $t_{1/2\beta}$, the apparent absorption and elimination half−life; MRT_{0-t}, mean residence time.

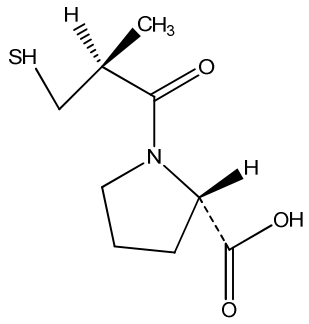

Fig. 1

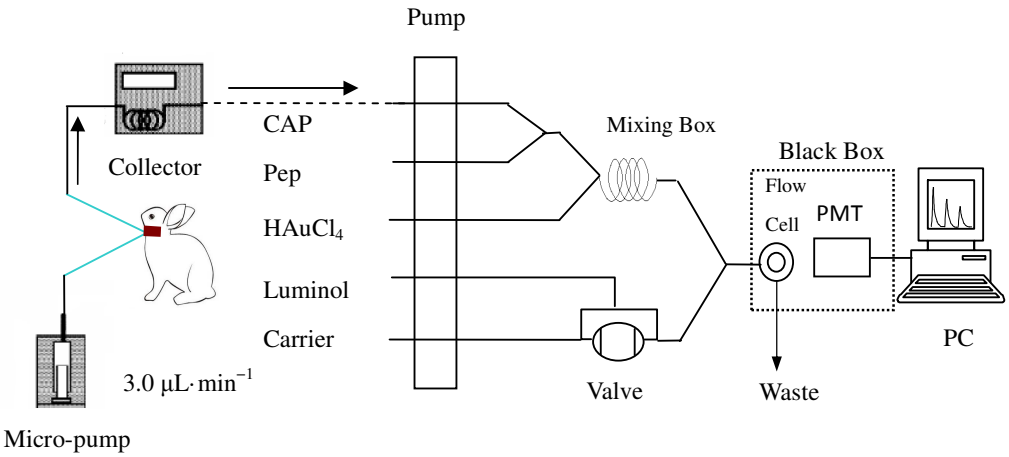

Fig. 2

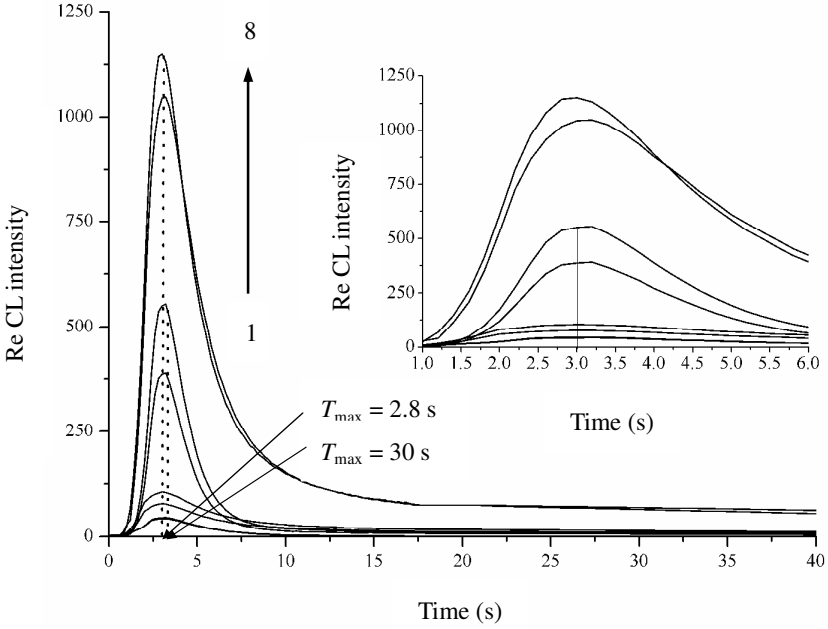

Fig. 3

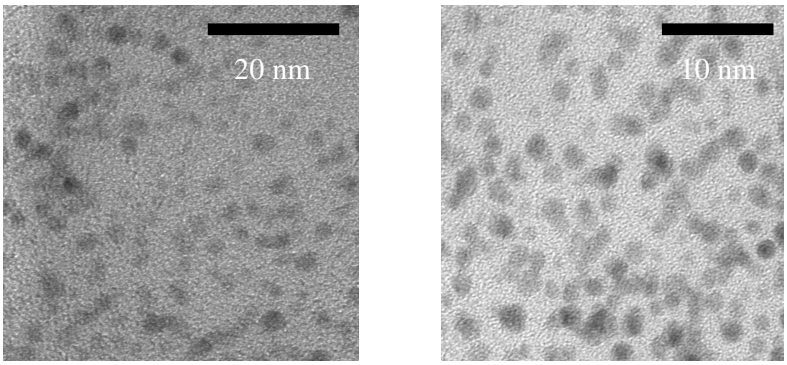

Fig. 4

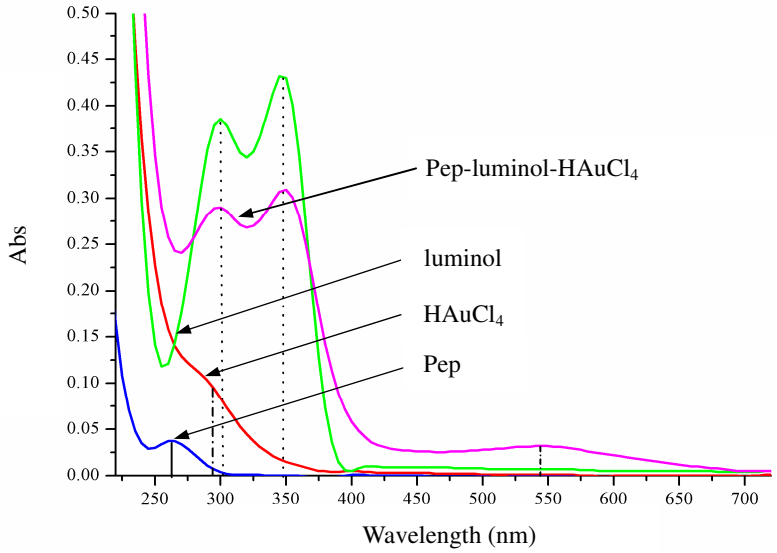

Fig. 5

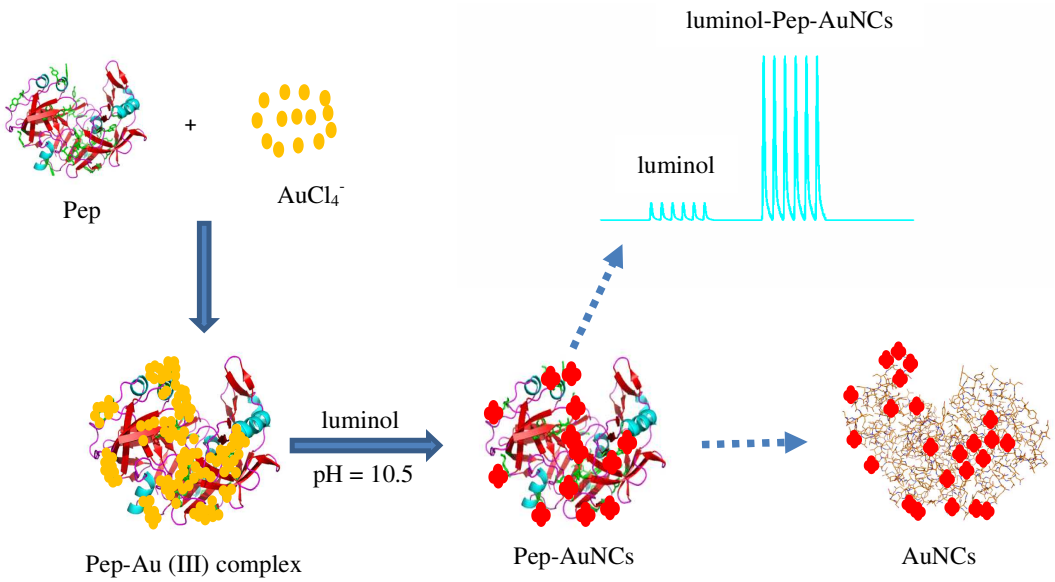

Fig. 6

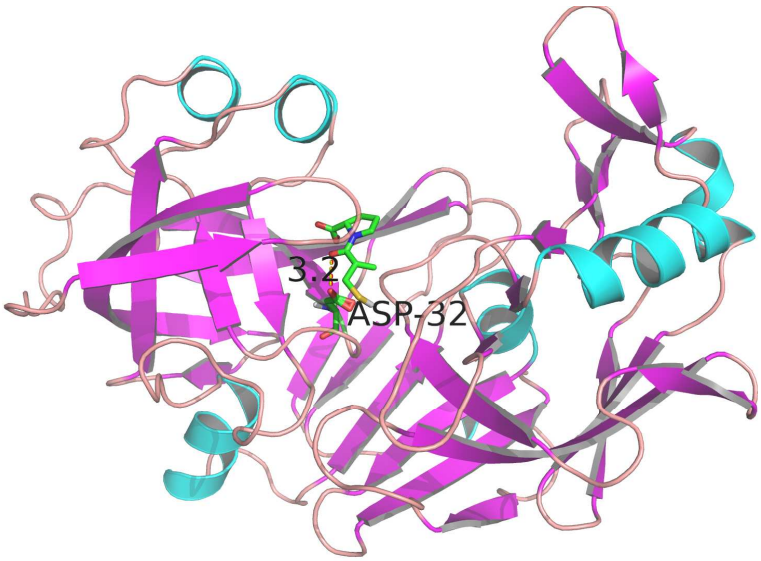

Fig. 7

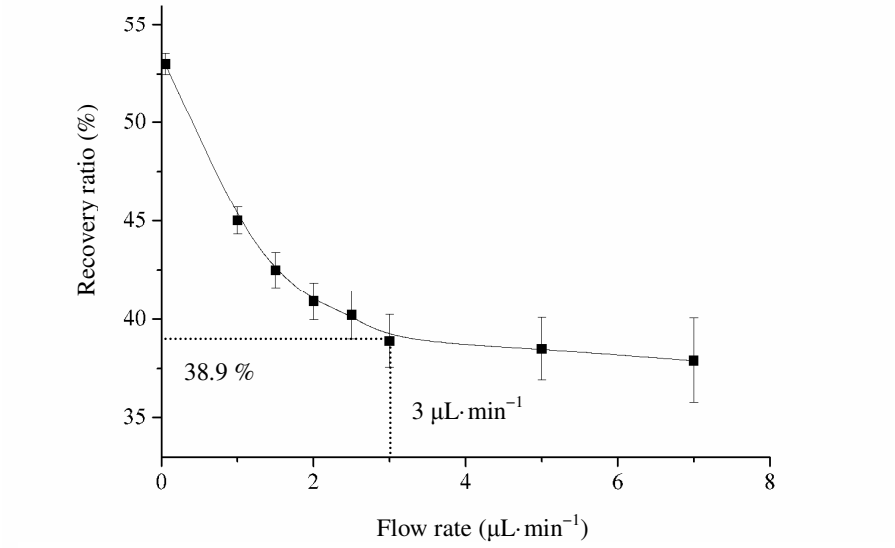

Fig. 8

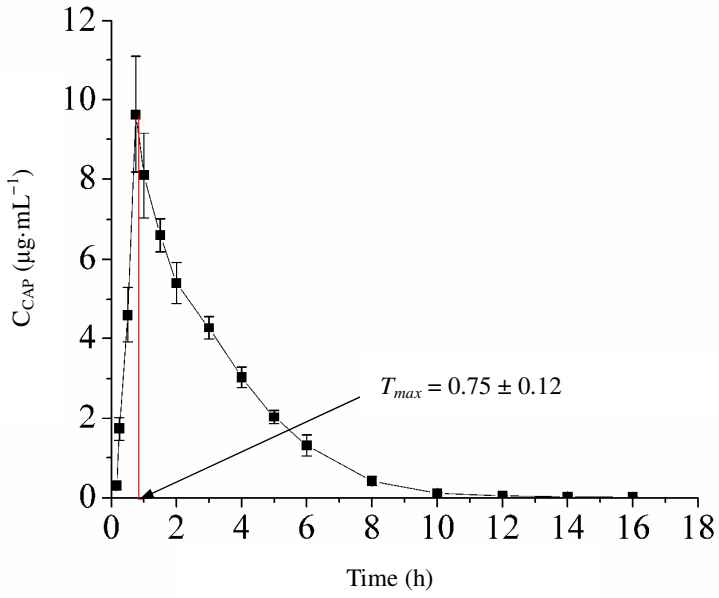

Fig. 9